Postcranial evidence of late Miocene hominin bipedalism in Chad

Franck Guy (franck.guy@univ-poitiers.fr)
Université de Poitiers / CNRS UMR 7262 - PALEVOPRIM Paléontologie, Evolution, Paléo-écosytèmes, Paléoprimatologie

Guillaume Daver
CNRS, UMR 7262

Hassane Taisso Mackaye
Université de N'Djamena

Andossa Likius
Université de N'Djamena - Faculté de Sciences Exactes et Appliquées -Département de Paléontologie

Jean-Renaud Boisserie
Université de Poitiers and CNRS

Abderamane Moussa
Université de N'Djamena - Faculté de Sciences Exactes et Appliquées -Département de Paléontologie

Patrick Vignaud
CNRS UMR 6046

Clarisse Nekoulnang
Centre National de Développement et de la Recherches (CNRD) - Service de Conservation et Valorisation des Fossiles

Research Article

Keywords: Terrestrial bipedal, Miocene hominins, postcranial remains

Posted Date: September 10th, 2020

DOI: https://doi.org/10.21203/rs.3.rs-69453/v1

Version of Record: A version of this preprint was published at Nature on August 24th, 2022. See the published version at https://doi.org/10.1038/s41586-022-04901-z.

Abstract

Terrestrial bipedal locomotion is one of the key adaptations defining the hominin clade. Evidences of undisputed bipedalism are known from postcranial remains of late Miocene hominins as soon as 6 Ma in eastern Africa. Bipedality of Sahelanthropus tchadensis was hitherto documented at 7 Ma in central Africa (Chad) by cranial evidence. Here, we present the first postcranial evidence of the locomotor behavior of the Chadian hominin with new insights on bipedalism at the early stage of our evolutionary history. The original material was discovered at locality TM 266 (Toros-Menalla fossiliferous area), and consists in one left femur and two antimeric ulnae. These new findings confirm that hominins were already terrestrial biped relatively soon after the human-chimpanzee divergence but also suggest that careful climbing arboreal behaviors was still a significant part of their locomotor repertoire.

Main Text

Discoveries in Chad by the Mission Paleoanthropological Franco-Tchadienne (MPFT) have substantially contributed to our understanding of early human evolution in Africa. The locality TM 266 (Extended data 1) in the Toros-Menalla fossiliferous area in the Mega-Chad basin yielded, among hundreds of vertebrate remains, a nearly complete cranium (TM 266-01-60-1), three mandibles, and several isolated teeth depicting a minimum of three adult individuals assigned to *Sahelanthropus tchadensis*[1,2]. TM 266 fossils were found in the Anthracotheriid Unit with biochronological estimates and radiochronological age at ca. 7 Ma[3,4]. Environmental indicators at Toros-Menalla localities, at the time, suggested a lacustrine fringe, in a desert vicinity, where open areas with dry and humid grasslands coexisted with arboreal cover[5,6].

Three other hominin fossil remains were discovered at TM 266 in 2001 by the MPFT: one left femoral shaft (TM 266-01-063, unearthed in July 2001), and two right and left ulnae (respectively TM 266-01-358, unearthed in November 2001 and TM 266-01-050, unearthed in July 2001; Supplementary notes). Despite none of these limb bones can be reliably ascribed to any hominin craniodental specimen found at TM 266, the most parsimonious hypothesis is that these postcranial remains belong to the sole hominin species present in this locality. Hence, we favor a conservative attribution of these specimens to *Sahelanthropus tchadensis*.

The hindlimb is documented by a left femoral shaft (TM 266-01-063) of about 242 mm long (Fig. 1 and Supporting table 1, Extended data 2), lacking the distal epiphysis and most of the proximal one. The specimen is curved anteroposteriorly as in *Australopithecus*[7-9] and *Orrorin tugenensis* (BAR 1002'00 and BAR 1003'00) but more heavily built. The two major mediolateral axes of the proximal and distal diaphyseal portions clearly indicate that the neck must have been anteverted as in fossil hominins[9-11] (Extended data 3). The presence of a groove on the postero-superior surface of the neck for the *obturator internus* and *m. gemelli* supports this interpretation. Resulting in head/neck torsion relative to the long axis of the shaft[12].This condition is also reported in archaic fossil apes such as *Nacholapithecus* and *Ekembo* but is absent in the arboreal biped *Danuvius*[13]. The femur exhibits proximal platymeria just distal to the lesser trochanter (Supplementary notes), a trait encountered in *O. tugenensis* and later hominins

and suggested to correlate with neck elongation, a reliable indicator of hominin bipedalism[9,14-16] (but see [8,17]). Concurrently, the neck is compressed antero-posteriorly as in the Miocene ape *Danuvius guggenmosi*[13] and hominins[8-9,18] (but see [19] for *Dryopithecus fontani* and *Hispanopithecus laietanus*; Fig. 1). This array of features agrees with habitual bipedalism in *S. tchadensis*.

A small but sharp relief, indicative of the third trochanter, continues into a rugose surface distally and blends with the lateral component of a broad 'proto-*linea aspera*'[17] (12.2mm in its narrowest width). The lateral lip of the *linea* forms a well-marked sigmoid line. Similarly, the medial lip of the *linea aspera* is well-marked. The spiral line for the insertion of the *vastus medialis* consists in a straight line, which confounds distally with the medial lip of the *linea aspera*. Such configuration is also observed in *O. tugenensis* and *Ardipithecus ramidus*[8,16,18] albeit with a more salient 'proto-linea aspera' in TM 266-01-063, but differs from modern humans where a pilaster develops. Such an overall pattern is consistent with bipedalism albeit suggesting a less-developed quadriceps system relative to the hamstring compared to modern human-like pattern[17].

The femoral shaft exhibits thick cortical bone in cross-section (Fig. 2). Cortical thickness distribution pattern describes a posterior and lateral thickening of the diaphysis relative to an anterior and medial thinning (Fig. 3). Posterior thickening of the cortical bone occurs at the level of the nutrient foramen, where the 'proto-*linea aspera*' is the narrowest. Conversely, extant apes share a posterior thickening on proximal half of the shaft and a relative thinning on distal half[20] (see also Supporting Information in [21]). Lateral thickening can be traced on the major part of the shaft in TM 266-01-063 except in its most distal portion. African apes do not display extended lateral thickening but instead, a circumscribed thickening corresponding to the lateral spiral pilaster. In these aspects, TM 266-01-063 most resembles extant humans. Comparative data are, to our knowledge, inexistent for *Ardipithecus*. Besides, cortical thickness data reported for BAR 1002'00 (*O. tugenensis)* rely on CT-scan data whose reliability is questionable[22-24].

Cortical area and second moment of area (I_x/Iy and I_{max}/I_{min} are biomechanical parameters frequently used to infer habitual locomotor functions in primates, as they reflect loads undergone by long bones during growth (but see [25]). The cortical area of the diaphyseal cross-section is a measure of resistance of the bone to axial compression or tension, while second moment of area measures the resistance to bending loads. In TM 266-01-063, percent of cortical area is 66.5 % at the level of the nutrient foramen (see Methods) and slightly increase proximally. It is within the range of extant and fossil apes (75 % ± 3.6 in extant humans; 63.3 % ± 7.6 in chimpanzees; 70 % ± 3.9 in gorillas; Supporting Information in [21]) and above the value reported for AL 288-1 femur (59.9 %) at midshaft[26]. Response to bending loads endured by the femur from TM 266 is assessed at the level of the nutrient foramen using second moment of area[26,27]. Results for I_{max}/I_{min} and I_x/I_y are respectively 1.31 and 0.81 (Extended data 4). The Chadian femur approaches the chimpanzee/extant human condition in its I_{max}/I_{min} ratio (measured at midshaft[28,29]; humans, I_{max}/I_{min}=1.6 ± 0.36; chimpanzees, I_{max}/I_{min}=1.4 ± 0.2) whereas it departs from gorillas[28] (I_{max}/I_{min}=1.9 ± 0.3). The I_x/I_y of TM 266-01-063 is close to values reported for chimpanzees

(chimpanzee[30]: I_x/I_y=0.75 ± 0.08), early *Homo*[31-33] and early to Middle Pleistocene hominins[34]. It departs from extant humans in which a posterior pilaster develops[29] (I_x/I_y =1.52 ± 0.39). Whereas midshaft cross-section of TM 266-01-063 resembles in its overall aspect to AL 288-1, the Chadian specimen present higher I_{max}/I_{min} and lower I_x/I_y values than its younger eastern-African relative (*A. afarensis*: AL 288-1[26], I_x/I_y=0.98 and I_{max}/I_{min}=1.07; see also [35] for AL 333-61, I_x/I_y=1.16 and I_{max}/I_{min}=1.16).

Many aspects such as stature, body mass, muscle attachment sites, positional behavior, ontogeny and sexual dimorphism[25] may contribute to femoral bone mass distribution. Yet, geometry of the TM 266-01-063 indicates greatest bending resistance for medio-laterally oriented stresses. This condition seen in AL 288-1 and early African and Asian *Homo* is suggested to relate to a more lateral position of the body during the stance phase of gait in association with an increase in femoral neck length and biacetabular breadth[26]. Functional interpretations remain difficult to formulate given the paucity of early hominin comparative data and given the state of preservation of the Chadian femur. Nevertheless, the Chadian femoral shaft exhibits a well-developed *calcar femorale* (CF) in its proximal portion (Fig. 4; the CF is 18.80 mm long measured at the level of the lesser trochanter following[36]), a condition to date only seen in extant humans and reported in *O. tugenensis* (BAR 1003'00). The *calcar femorale* corresponds to a bony wall that originates from the postero-medial endosteal surface at the level of the lesser trochanter and extends laterally toward the greater trochanter. In obligate bipeds, it facilitates compressive loads dispelling in the proximal femur by decreasing the stress in the posterior and medial aspects and increasing the stress in the anterior and lateral aspects[36,37]. A well-developed *calcar femorale* in TM 266-01-063 represents a morphological requirement for terrestrial bipedalism.

The forearm bones attributed to *Sahelanthropus tchadensis* consist in two partial left and right ulnae lacking the distal epiphyses. Similarity in size and shape for the antimeric ulnae could suggest they are from the same individual, even if no definitive evidence supports this assumption. TM 266-01-050 is a left ulnar diaphysis of 239 mm long (Fig. 5, Supporting table 1, Extended data 2) showing eroded proximal epiphysis. The right ulna (TM 266-01-358) corresponds to a proximal-half shaft of 155 mm long with partially preserved epiphysis. The shafts are curved in profile. Similar anteroposterior curvature is observed in *Ar. kadabba*[38] (ALA-VP 2/101) and later hominins StW 573k and OH 36, as in extant apes[9,39,40]. This feature contrasts with the straight right ulnar shafts of *D. guggenmosi* and *A. prometheus,* but this lack of curvature is likely due to a pathological condition[9,13]. In primates, such ulnar curvature is due to habitual loads exerted by the action of m. *brachialis* in order to maintain elbow flexion in arboreal context, which in turn involves the antagonistic action of a powerful forearm musculature, including wrist and fingers extensors and flexors[40,41].

The preserved flat distal portion of the olecranons indicate that they were not projecting posteriorly as in extant African apes[42]. In this regard, the distal portion of the olecranon most resembles the condition seen in Miocene apes[42-44] and in hominins[42]. The proximal epiphyses indicates an anteriorly-facing trochlear notch as in fossil hominins and Miocene apes[9,13,42-45]. Hence, the Toros-Menalla ulnae depart

from the typical proximally oriented trochlear notch in extant great apes[41,46]. In functional terms, a more anteriorly facing notch, associated with an olecranon aligned with the long axis of the forearm, favors triceps leverage at mid-flexion[41,46]. In *Ar. ramidus* such function is linked to careful climbing and bridging[44]. Conversely, a more proximally facing notch reflects differential loading during suspension[43] while a posteriorly projecting olecranon favors triceps leverage in extension and is commonly associated with terrestrial quadrupedal locomotion in anthropoids[42].

Ulnae from Toros-Menalla display a keeled trochlear notch with a comparatively acute angle relative to later hominins and African apes. The distal keeling angle, measured from TM 266-01-358 (distal keeling angle=109°), is in the lower range of *Pongo pygmaeus* and close to the value reported for *Oreopithecus bambolii* and the left ulna AL 288-1t in *A. afarensis*[46]. Likewise, the proximal angle is acute (proximal keeling angle=100°), in the lower range of reported values for chimpanzees, and close to OH 36 and *Or. bambolii*[46]. A pronounced trochlear keel warrants medio-lateral stability of the elbow in response to powerful superficial finger and wrist flexors, and forearm pronator (*mm flexor digitorum superficialis*, *flexor carpi radialis* and *ulnaris*, and *pronator teres*)[39,46]. Such configuration was supposedly reported on *D. guggenmosi*[13] and is typical of the arboreal large apes, which integrates climbing, and/or suspension in their locomotor repertoire[46]. It is unlikely to reflect habitual terrestrial quadrupedalism. The TM 266 ulnae lack prominent flexor apparatus entheses as in orangutans, *Ar. ramidus* and later hominins. In this respect, it differs from the condition seen in Miocene apes and extant quadrupedal monkeys. Such morphology precludes the possibility of quadrupedalism and, more specifically, of knuckle-walking as primary locomotor behaviors for the Toros-Menalla hominins[45].

Overall, the trochlear notch of TM 266 ulnae present an unusual morphology as the middle portion is mediolaterally narrow relative to the distal half. This waisted aspect of the trochlear notch approaches the condition seen in 'small' apes (humans, chimpanzees and bonobos) and contrasts with that of 'large' apes (orangutans and gorillas). Such configuration is interpreted as locomotor-independent and rather linked to allometry[46]. The disto-medial quadrant of TM 266-01-358 is clearly more developed than the distolateral one, an intermediate morphology between humans and chimpanzees, close to that of *D. guggenmosi*[13], *A. afarensis*, and *A. prometheus*[9,46]. A developed medial portion of the trochlear notch is an adaptation for maximum joint compression medially, a configuration which could meet mechanical requirements in various non terrestrial locomotor behaviors[13,46].

Only limited portions, proximally and distally, of TM 266-01-050 allow assessing cortical bone distribution (see Supplementary notes, Extended data 4). Proximally, the percent of cortical area is 73.4 %, measured at about 70-75 % of the estimated total lengths of the ulna (see methods). At mid-shaft, the percent of cortical area is 81.0 %, falling within the variation of Late Pleistocene hominins (80.1 % ± 6.6 in *H. sapiens* and 82.8 % ± 7.1 in neandertals)[47]. Besides, I_{max}/I_{min} and I_x/I_y are respectively 2.04/1.62 at 70-75 % level and 1.71/1.13 at midshaft. Values for the Chadian ulna fall outside the reported variation for gorillas[48] and is within the range of variation in chimpanzees for proximal I_{max}/I_{min} and proximal-

midshaft I_x/I_y. Besides, TM 266-01-050 is within the range of variation of Asian non-human apes for all ratios except for the lower measured proximal I_{max}/I_{min} in *Pongo*. The geometry of TM 266-01-050 deviates from circularity in the antero-posterior direction. The cortical bone is predominantly distributed antero-posteriorly as in orangutans and to a lesser extent in chimpanzees. This condition contrasts with the one seen in gorillas, which tend to grow more bone medio-laterally. Relative medio-lateral expansion is suggested to adjust for increased vertical and medio-lateral forces that apply to the forelimb in terrestrial quadrupedal primates[45,49,50]. Besides, considering comparative data available for chimpanzees and orangutans, which tend to grow more bone antero-posteriorly[51], the Chadian ulna configuration more likely reflects bending loads associated with a wide array of arboreal locomotor modes. Yet, the TM forelimb bones lack any traits typical of suspension or knuckle walking, and exhibit a configuration better seen in apes engaged in careful climbing[44]. However, the possibility that the Chadian hominin was capable of vertical climbing cannot be dismissed given the particularly keeled trochlear notch.

The Toros-Menalla femur exhibits several hallmarks of habitual terrestrial bipedalism. Among them, a well-defined broad proto-*linea aspera,* the presence of a lateral third trochanter and associated subtrochanteric platymeria without hypotrochanteric or infero-lateral fossae, is classically associated with enhanced hip flexion-extension[16,20,52], while a particularly developed *calcar femorale* facilitates compressive loads dispelling in terrestrial bipedalism[36]. These features go with an overall cortical bone distribution pattern and cross-section geometries of the femoral shaft that suggest muscular recruitments and bone loads compatibles with habitual bipedalism. Despite some of the above-mentioned traits are suggested to be the primitive condition in hominins (proximal platymeria or gluteal tuberosity)[17], they are part of a functional complex co-opted for bipedalism. They are routinely considered as such to infer potential bipedal terrestrial locomotion in early eastern African hominins[7,8,16,18,52,53]. The Chadian hindlimb bone conforms to the overall morphological pattern of Miocene hominin terrestrial bipeds. The forelimbs morphology rules out arboreal specialization for the Chadian material, as in *Ar. ramidus*[16] and presumably *O. tugenensis*[7]. Yet, the Chadian postcranial material displays a suite of morphological features that are consistent with substantial non-stereotypical arboreal behaviors, as suggested by ulnar shaft curvature and cross-section geometrical properties, whereas the elbow morphology is potentially indicative of careful climbing[44], and does not display any evidence of knuckle-walking.

Recently, it was suggested that the putative stem hominid *D. guggenmosi* was able to use obligate arboreal bipedalism combined to suspension as early as the late middle Miocene[13]. The authors suggested that hominin terrestrial bipedalism and great ape suspension evolved from such locomotor repertoire[13]. In the lack of evidence supporting a phylogenetic relationship between hominins and Miocene European apes, we cannot infer that hominin terrestrial bipedalism originated from middle Miocene forms in Europe as suggested by [13]. Instead, the Chadian remains described herein reassert African roots. They are the first direct evidence of an obligate terrestrial bipedalism, indistinguishable from that inferred for *O. tugenensis* and *Ar. kadabba*/*ramidus*. They suggest a precocious adaptation to

bipedalism after the human-chimp dichotomy[54]. The Chadian remains suggests a conservative evolution of climbing capacities, interpreted as cautious climbing as in stem apes[54]. Hence, cautious climbing modality weakens a potential role of suspension in the emergence of the hominin clade[13].

The Toros-Menalla postcranial material also reasserts the presence of cladistic hominins in the upper Miocene of Chad, within particular environmental settings. Eastern African Miocene hominins are associated with open woodland areas with significant tree cover at ~6 Ma at Lukeino[55], and a mixture of woodland combined with wet grassland for the earliest postcranial-based bipedalism occurrence in Ethiopia at 5.2 Ma (AME-VP-1/71, *Ardipithecus kadabba*)[38,56]. At 4.4 Ma, *Ar. ramidus* most probably inhabited a ground-water-fed grassy woodland (probably a palm grove) at Aramis[57-58].

Taken as a whole, eastern-African early hominins share an arboreal component in their habitat (see [57,59] for discussion on Aramis). Environmental indicators in Toros-Menalla fossiliferous area suggest heterogeneous landscape types consisting of closed forest formations (probably riparian forests), palm grove formations, and mixed/grassland formations (from woodlands to savannas/aquatic grasslands)[5,6,60]. Therefore, the Chadian hominins were probably no exception as being reliant on arboreal cover given their potential climbing abilities. As bipeds, they were not exclusive arboreal forest dwellers, because they were able to raid in near open environments for food/water resource harvesting. The association between a polyvalent locomotion (arboreality and bipedal terrestriality), and wooded formations in mesic context during at least ~2.5 million years suggests that the ecological niche of these early hominins was not strongly tied to the expansion of relatively dry, open areas. This niche could be depicted as opportunistic in its reliance on both terrestrial and arboreal resources.

Based on molecular data, the chimpanzee-human last common ancestor (CHCLA) is estimated to occur in Africa between 10 and 7 Ma[61,62]. Indeed, fossil representatives of the panin clade are too scarce and consists in a minimum of three Middle Pleistocene teeth from the Kapthurin formation in Kenya[63] and a chimpanzee-like proximal femoral epiphysis of unknown age from the Kikorongo crater in Uganda[64]. However, at least three taxa have been described between 10 Ma and 7 Ma in African deposits: *Samburupithecus*, from Samburu Hills, around 9.5 Ma[65], *Nakalipithecus* from Nakali, around 9,8 Ma[66] and *Chororapithecus* from the Middle Awash, around 8 Ma[62,67]. These Miocene taxa are parsimoniously assigned to stem hominines[68,69], even if *Samburupithecus* displays a particularly archaic morphology[69]. *Chororapithecus* displays derived dental affinities with *Gorilla*[67]. In light of this record and of the lack of phylogenetic resolution, the ancestral condition of positional behaviour in African apes and humans will remain elusive until significant new data becomes available. To date, the identification of the derived traits shared by hominins relies on the analysis of the earliest forms of the clade. The early hominins *Sahelanthropus, Orrorin* and *Ardipithecus* share the same combination of non-honing C-P3 complex and of features linked to terrestrial bipedalism. This combination is arguably more similar to the condition observed in later hominins than in any other African fossil or extant hominoids. This is currently the only data available for formulating scenarios about the latest Miocene/earliest Pliocene evolution of African hominoids. In absence of Mio-Pliocene fossils displaying exclusive morphological affinities with *Pan*,

cautionary tales about rampant homoplasy and character polarity in this evolutionary sequence[70] are poorly suitable to falsification attempts. Instead, the morphological homogeneity of the purported hominids implies that the interpretation of the combined non-honing C-P3 complex-bipedal hindlimb as a synapomorphic signature of early hominids currently remains the most parsimonious hypothesis

Methods

The original fossil specimens are measured to the nearest 0.1 mm using a Mitutoyo sliding digital caliper.

Computed tomography

High-resolution micro-computed tomography (HR-mCT) images taken from the original femur and ulnae were used to assess the inner morphology of the bones. The material was scanned with EasyTom XL Duo mCT (using a sealed Hamamatsu microfocus x-ray source - 75 W, 150 kV - and an amorphous silicon based detector Varian PaxScan 2520DX, 1536*1920 pixel matrix; 127 mm pixel pitch, 16 bits, CsI conversion screen - from RX-Solutions, France) at Plateforme PLATINA (University of Poitiers). For scanning procedures, beam intensity was set at 90 kV and tube current at 333 mA. The TM 266- 01-358 ulna was acquired with 3584 projections resulting in 3036 slices of 730*825 pixels using a cone-beam reconstruction algorithm. The isovoxel size was set to 0.0525 mm. The TM 266-01-050 ulna was acquired with 4800 projections resulting in 4051 slices of 589*849 pixels. The isovoxel size was set to 0.0600 mm. The TM 266-01-063 femur was acquired with 5984 projections resulting in 4962 slices of 1162*911 pixels. The isovoxel size was set to 0.0499 mm.

Virtual models processing

Semi-automatic segmentation of the virtual fossil specimens and three-dimensional surfaces extraction were performed in Avizo Lite. Three-dimensional surfaces were prepared and treated using Geomagic Studio. Cortical bone thickness distribution was assessed in three dimensions using the *Surface thickness* module in Avizo Lite from the outer surface of the of the segmented medullar cavity to the outer surface of the femur. All measurements based on 3D virtual models of the fossil specimen were done in Avizo Lite on 3D volumes and Fiji image software[71] on 2D slices.

Cross-sectional geometric properties (CSGP)

The femur lacks the most part of the epiphyses, which prevents from estimating its biomechanical length. However, CSGP values in *Homo* and *Pan* do no show significant differences between 45-55 % of the femoral (biomechanical or maximum) length[31]. Comparison of diaphyseal cross-sectional geometry from fragmentary specimens must be evaluated on a case-by-case basis[31]. Superimposition of the femora BAR 1002'00 (*O. tugenensis*) and TM 266-01-063 using the distal base of their lesser trochanter (corresponding to 80 % of the biomechanical length[72]), show that the nutrient foramen on TM 266-01-063 provides a reliable indicator of the midshaft level. CSGP estimates were computed at nutrient foramen level and then, in order to get an assessment of the variation pattern of cortical bone distribution, at four

additional cross-sections, equally spaced from the nutrient foramen to the base of the lesser trochanter. For ulnae, CSGP variables were computed proximally from 35.0 mm below the distal border of the radial notch (and at the level of the nutrient foramen), which corresponds to 70-75 % of the estimated ulna length for TM 266-01-050 (estimated using OMO L40-19 fossil hominin ulna as analog).

Percentage of cortical area and second moment of area were computed using Fiji image software[71] and BoneJ plugin[73].

Comparative data for CSGP with extant and extinct hominoids (Extended data 4) were gathered from [19,21,26,28-30,32,33,35,74,75].

71. Schindelin, J. et al. Fiji: an open-source platform for biological-image analysis. Nature methods **9**, 676-682 (2012).
72. Ruff, C. B. Long bone articular and diaphyseal structure in Old World monkeys and apes. I: locomotor effects. *Am. J. Phys. Anthrop.* **119**, 305-342 (2002)
73. 73. Doube, M. *et al.* BoneJ: Free and extensible bone image analysis in ImageJ. *Bone* **47**, 1076-1079 (2010).
74. MaClatchy, L., Gebo, D., Kityo, R., & Pilbeam, D. Postcranial functional morphology of *Morotopithecus bishopi*, with implications for the evolution of modern ape locomotion. *J. Hum. Evol.* **39**, 159-183 (2000).
75. Rodríguez, L., Carretero, J. M., García-González, R., & Arsuaga, J. L. Cross-sectional properties of the lower limb long bones in the Middle Pleistocene Sima de los Huesos sample (Sierra de Atapuerca, Spain). *J. Hum. Evol.* **117**, 1-12 (2018).

Declarations

Author contributions

G.D. and F. G. designed the study, collected and interpreted the data. G.D., F.G. and J.-R. B. wrote the manuscript. G. D., F. G., J.-R. B., M.H.T., A.L., M.A., P.V. and C.N. discussed the results and revised earlier drafts of the papers.

Acknowledgments

We thank the Chadian Authorities (Ministère de l'Education Nationale de l'Enseignement Supérieur, de la Recherche et de l'Innovation, Université de Djamena & CNRD). We extend gratitude for their support to the French Ministries, Ministère Français de l'Education Nationale (Collège de France, Université de Poitiers), Ministère de la Recherche (CNRS), Ministère de l'Europe et des affaires étrangères (Direction de la

Coopération Scientifique, Universitaire et de Recherche, Paris, and SCAC Ambassade de France à N'djamena, Commission de Consultation des recherches Archéologiques à l'Etranger), to the Région Nouvelle Aquitaine, and also to the Armée Française (MAM, Epervier and Barkhane) for logistic support. We would like to thank deeply to Professor M. Brunet, head of the M.P.F.T., who initiated this work and gathered the first comparative data at the basis of the present manuscript. For giving him the opportunity to work with their collections, we are grateful to our Colleagues and their Institutions: C.O. Lovejoy (Kent State University), B. Asfaw (National Museum of Ethiopia), Y. Haile-Selassie (Cleveland Museum of Natural History), M. G. Leakey & R. Leakey (National Museum of Kenya), D. Pilbeam (Peabody Museum and Harvard University), D. Johanson & W. Kimbel (Institute of Human Origins and Arizona State University at Tempe), T. White (University of California at Berkeley) and G. Suwa (University Museum of Tokyo). Special thanks to all our colleagues and friends for their help and discussion, and particularly to D. Barboni, A. Mazurier (Centre de Microtomographie), A. Novello. We especially thank all the MPFT members who participated to the field missions, and Ahounta D., Fanoné G. (deceased), Mahamat A., S. Riffaut, J. Surault and X. Valentin for technical support. We are most grateful to G. Florent, C. Noël, G. Reynaud, C. Baron, M. Pourade, and L. Painault for administrative guidance.

References

1. Brunet, M. *et al.* A new hominid from the Upper Miocene of Chad, Central Africa. *Nature* **418**, 145–151 (2002).
2. Brunet, M. *et al.* New material of the earliest hominid from the Upper Miocene of Chad. *Nature* **434**, 752–755 (2005).
3. Vignaud, P. *et al.* Geology and palaeontology of the Upper Miocene Toros-Menalla hominid locality, Chad. *Nature* **418**, 152–155 (2002).
4. Lebatard, A. E. *et al.* Cosmogenic nuclide dating of *Sahelanthropus tchadensis* and *Australopithecus bahrelghazali*: Mio-Pliocene hominids from Chad. *Proc. Natl. Acad. Sci. USA* **105**, 3226–3231 (2008).
5. Le Fur, S., Fara, E., Mackaye, H. T., Vignaud, P., & Brunet, M. The mammal assemblage of the hominid site TM266 (Late Miocene, Chad Basin): ecological structure and paleoenvironmental implications. *Naturwissenschaften* **96**, 565–574 (2009).
6. Schuster, M. *et al.* Chad Basin: paleoenvironments of the Sahara since the Late Miocene. *C. R. Geosci.* **341**, 603–611 (2009).
7. Senut, B. *et al.* First hominid from the Miocene (Lukeino formation, Kenya). *C. R. Acad. Sci. Paris IIA* **332**, 137–144 (2001).
8. Pickford, M., Senut, B., Gommery, D., & Treil, J. Bipedalism in *Orrorin tugenensis* revealed by its femora. *C. R. Palevol* **1**, 191–203 (2002).
9. Heaton, J. L. *et al.* The long limb bones of the StW 573 *Australopithecus* skeleton from Sterkfontein Member 2: Descriptions and proportions. *J. Hum. Evol.* **133**, 167–197 (2019).
10. Lovejoy, C. O., Cohn, M. J., & White, T. D. Morphological analysis of the mammalian postcranium: a developmental perspective. *PNAS*, **96**, 13247–13252 (1999).

11. Tardieu, C. Development of the human hind limb and its importance for the evolution of bipedalism. *Evol Anthrop: Issues, News, and Reviews*, **19**, 174–186 (2010).
12. Marchi, D. *et al.* The thigh and leg of Homo naledi. *J. Hum. Evol.* **104**, 174–204 (2017).
13. Böhme, M. *et al.* A new Miocene ape and locomotion in the ancestor of great apes and humans. *Nature*, **575**, 489–493 (2019).
14. Ruff, C. in *Primate Locomotion: Recent Advances* (eds. Strasser, E., Fleagle, J., Rosenberger, A.L., & McHenry, H.) 449–469 (Springer, Boston, MA, 1998).
15. Lovejoy, C. O., Meindl, R. S., Ohman, J. C., Heiple, K. G., & White, T. D. The Maka femur and its bearing on the antiquity of human walking: applying contemporary concepts of morphogenesis to the human fossil record. *Am. J. Phys. Anthropol.* **119**, 97–133 (2002).
16. Lovejoy, C. O., Suwa, G., Spurlock, L., Asfaw, B., & White, T. D. The pelvis and femur of *Ardipithecus ramidus*: the emergence of upright walking. *Science* **326**, 71e1-71e6 (2009).
17. Almécija, S. *et al.* The femur of *Orrorin tugenensis* exhibits morphometric affinities with both Miocene apes and later hominins. *Nat. Commun.* **4**, 2888 (2013).
18. Richmond, B. G., & Jungers, W. L. *Orrorin tugenensis* femoral morphology and the evolution of hominin bipedalism. *Science* **319**, 1662–1665 (2008).
19. Pina, M. *Unravelling the positional behaviour of fossil hominoids morphofunctional and structural analysis of the primate hindlimb*. Doctoral dissertation, Universitat Autònoma de Barcelona (2016).
20. Morimoto, N., De León, M. S. P., Nishimura, T., & Zollikofer, C. P. Femoral morphology and femoropelvic musculoskeletal anatomy of humans and great apes: a comparative virtopsy study. *Anat. Rec.* **294**, 1433–1445 (2011).
21. Macchiarelli, R. & Zanolli, C. Hominin biomechanics, virtual anatomy and inner structural morphology: From head to toe. A tribute to Laurent Puymerail. *C. R. Palevol* **16**, 493–498 (2017).
22. Eckhardt, R. B., Galik, G., & Kuperavage, A. J. Questions about *Orrorin* femur: response. *Science* **307**, 845 (2005).
23. Galik, K. *et al.* External and internal morphology of the BAR 1002'00 *Orrorin tugenensis* femur. *Science 305*, 1450–1453 (2004).
24. Ohman, J. C., Lovejoy, C. O., & White, T. D. Questions about *Orrorin* femur. *Science* **307**, 845 (2005).
25. Lieberman, D. E., Polk, J. D., & Demes, B. Predicting long bone loading from cross-sectional geometry. *Am. J. Phys. Anthropol.* **123**, 156–171 (2004).
26. Ruff, C. B., Burgess, M. L., Ketcham, R. A., & Kappelman, J. Limb Bone Structural Proportions and Locomotor Behavior in AL 288-1 (" Lucy"). *PLoS ONE* **11**, e0166095 (2016).
27. Lovejoy, C. O., Burstein, A. H., & Heiple, K. G. The biomechanical analysis of bone strength: a method and its application to platycnemia. *Am. J. Phys. Anthropol.* **44**, 489–505 (1976).
28. Mongle, C. S., Wallace, I. J. & Grine, F. E. Cross-sectional structural variation relative to midshaft along hominine diaphyses. II. The hind limb. *Am. J. Phys. Anthropol.* **158**, 398–407 (2015).

29. Trinkaus, E. & Ruff, C. B. Femoral and Tibial Diaphyseal Cross-Sectional Geometry in Pleistocene *Homo*. *PaleoAnthropology* 2012, 13–62 (2012).
30. Nadell, J. *Ontogeny and Adaptation: A Cross-Sectional Study of Primate Limb Elements*. Doctoral dissertation, Durham University (2017).
31. Puymerail, L. *et al.* Structural analysis of the Kresna 11 *Homo erectus* femoral shaft (Sangiran, Java). *J. Hum. Evol.* **63**, 741–749 (2012).
32. Ruff, C. Femoral/humeral strength in early African *Homo erectus*. *J. Hum. Evol.* **54**, 383–390 (2008).
33. Ruff, C. Relative limb strength and locomotion in *Homo habilis*. *Am. J. Phys. Anthropol.* **138**, 90–100 (2009).
34. Ruff, C. B., Puymerail, L., Macchiarelli, R., Sipla, J., & Ciochon, R. L. Structure and composition of the Trinil femora: functional and taxonomic implications. *J. Hum. Evol.* **80**, 147–158 (2015).
35. Chevalier, T. AL 333 – 61 femoral diaphysis: evidence of obligate bipedalism 3.2 million years ago in Ethiopia? *Bull. Mém. Soc. Anthropol. Paris* **25**:169–189 (2013).
36. Kuperavage, A., Pokrajac, D., Chavanaves, S. & Eckhardt, R. B. Earliest known hominin *calcar femorale* in *Orrorin tugenensis* provides further internal anatomical evidence for origin of human bipedal locomotion. *Anat. Rec.* **301**, 1834–1839 (2018).
37. Zhang, Q. *et al*. The role of the *calcar femorale* in stress distribution in the proximal femur. *Orthop. surg.*, **1**, 311–316 (2009).
38. Haile-Selassie, Y., Suwa, G. & White, T. in *Ardipithecus kadabba: Late Miocene Evidence From The Middle Awash, Ethiopia* (eds. Haile-Selassie, Y., & WoldeGabriel, G.) 159–236 (Univ of California Press, 2009).
39. Drapeau, M. S. M., Ward, C. V., Kimbel, W. H., Johanson, D. C., & Rak, Y. Associated cranial and forelimb remains attributed to *Australopithecus afarensis* from Hadar, Ethiopia. *J. Hum. Evol.* **48**, 593–642 (2005).
40. Henderson, K., Pantinople, J., McCabe, K., Richards, H. L. & Milne, N. Forelimb bone curvature in terrestrial and arboreal mammals. *PeerJ* **5**, e3229 (2017).
41. Drapeau, M. S. M. Functional anatomy of the olecranon process in hominoids and Plio-Pleistocene hominins. *Am. J. Phys. Anthropol.* **124**, 297–314 (2004).
42. Begun, D. R. Phyletic diversity and locomotion in primitive European hominids. *Am. J. Phys. Anthropol.* **87**, 311–340 (1992).
43. Takano, T. *et al.* Forelimb long bones of *Nacholapithecus* (KNM-BG 35250) from the middle Miocene in Nachola, northern Kenya. *Anthropol. Sci.* **126**, 135–149 (2018).
44. Lovejoy, C. O., Simpson, S. W., White, T. D., Asfaw, B., & Suwa, G. Careful climbing in the Miocene: the forelimbs of *Ardipithecus ramidus* and humans are primitive. *Science* **326**, 70e1-70e8 (2009).
45. Alba, D. M., Almécija, S., Casanovas-Vilar, I., Méndez, J. M., & Moyà-Solà, S. A partial skeleton of the fossil great ape *Hispanopithecus laietanus* from Can Feu and the mosaic evolution of crown-hominoid positional behaviors. *PLoS ONE* **7**, e39617 (2012).

46. Drapeau, M. S. M. Articular morphology of the proximal ulna in extant and fossil hominoids and hominins. *J. Hum. Evol.* **55**, 86–102 (2008).
47. Churchill, S. E. *et al.* Morphological affinities of the proximal ulna from Klasies River main site: archaic or modern? *J. Hum. Evol.* 31, 213–237 (1996).
48. Nadell, J.A. Ontogeny and adaptation: a cross-sectional study of primate limb elements, Doctoral dissertation, Durham University (2017).
49. Carlson, K.J. et al. Role of nonbehavioral factors in adjusting long bone diaphyseal structure in free-ranging Pan troglodytes. *Int. J. Primatol.* **29**, 1401–1420 (2008).
50. Schmitt, D. Mediolateral reaction forces and forelimb anatomy in quadrupedal primates: implications for interpreting locomotor behavior in fossil primates. *J. Hum. Evol.* **44**, 47–58 (2003).
51. Morimoto, N. *et al.* Let bone and muscle talk together: a study of real and virtual dissection and its implications for femoral musculoskeletal structure of chimpanzees. *J. Anat.* **226**, 258–267 (2015).
52. White, T. D. *et al.* Asa Issie, Aramis and the origin of *Australopithecus*. *Nature* **440**, 883–889 (2006).
53. Ward, C. V., Kimbel, W. H., Harmon, E. H. & Johanson, D. C. New postcranial fossils of *Australopithecus afarensis* from Hadar, Ethiopia (1990–2007). *J. Hum. Evol.* **63**, 1–51 (2012).
54. Lovejoy, C. O. et al. The great divides: Ardipithecus ramidus reveals the postcrania of our last common ancestors with African apes. *Science* **326**, 73–106 (2009).
55. Bamford, M. K., Senut, B. & Pickford, M. Fossil leaves from Lukeino, a 6-million-year-old Formation in the Baringo Basin, Kenya. *Geobios* **46**, 253–272 (2013).
56. WoldeGabriel, G. et al. Geology and palaeontology of the late Miocene Middle Awash valley, Afar rift, Ethiopia. *Nature* **412**, 175–178 (2001).
57. White, T. D. *et al.* Macrovertebrate paleontology and the Pliocene habitat of *Ardipithecus ramidus*. *Science* **326**, 67–93 (2009).
58. Barboni, D., Ashley, G. M., Bourel, B., Arraiz, H. & Mazur, J. C. Springs, palm groves, and the record of early hominins in Africa. *Rev. Palaeobot. Palynol.* **266**, 23–41 (2019).
59. Cerling, T. E. *et al.* Woody cover and hominin environments in the past 6 million years. *Nature* **476**, 51–56 (2011).
60. Novello, A. *et al.* Phytoliths indicate significant arboreal cover at *Sahelanthropus* type locality TM266 in northern Chad and a decrease in later sites. *J. Hum. Evol.* **106**, 66–83 (2017).
61. Steiper, M. E. & Young, N. M. Timing primate evolution: lessons from the discordance between molecular and paleontological estimates. *Evol. Anthropol.* **17**, 179–188 (2008).
62. Katoh, S. *et al.* New geological and palaeontological age constraint for the gorilla–human lineage split. *Nature* **530**, 215–218 (2016).
63. McBrearty, S. & Jablonski, N. G. First fossil chimpanzee. *Nature 437*, 105–108 (2005).
64. DeSilva, J., Shoreman, E. & MacLatchy, L. A fossil hominoid proximal femur from Kikorongo Crater, southwestern Uganda. *J. Hum. Evol. 50*, 687–695 (2006).

65. Ishida H. & Pickford M. A new late Miocene hominoid from Kenya: *Samburupithecus kiptalami gen.* et sp. nov. *C.R. Acad. Sci. Paris* **325**,823–829 (1997).
66. Kunimatsu, Y. et al. A new Late Miocene great ape from Kenya and its implications for the origins of African great apes and humans. Proc. Natl Acad. Sci. USA **104**, 19220–19225 (2007).
67. Suwa G., Kono R.T., Katoh S., Asfaw B. & Beyene Y. A new species of great ape from the late Miocene epoch in Ethiopia. *Nature* **448**, 921–924 (2007).
68. Harrison, T. in Cenozoic Mammals of Africa (eds. Werdelin, L. & Sanders,W.J.) 429–469 (Univ of California Press, Berkeley, 2010).
69. Begun, D.R. in Handbook of Paleoanthropology, (eds. Henke, W. & Tattersall, I.) 1261–1332 (Springer-Verlag, Berlin Heidelberg, 2015)
70. Wood, B. & Harrison, T. The evolutionary context of the first hominins. *Nature* **470**: 347–352 (2011).

Figures

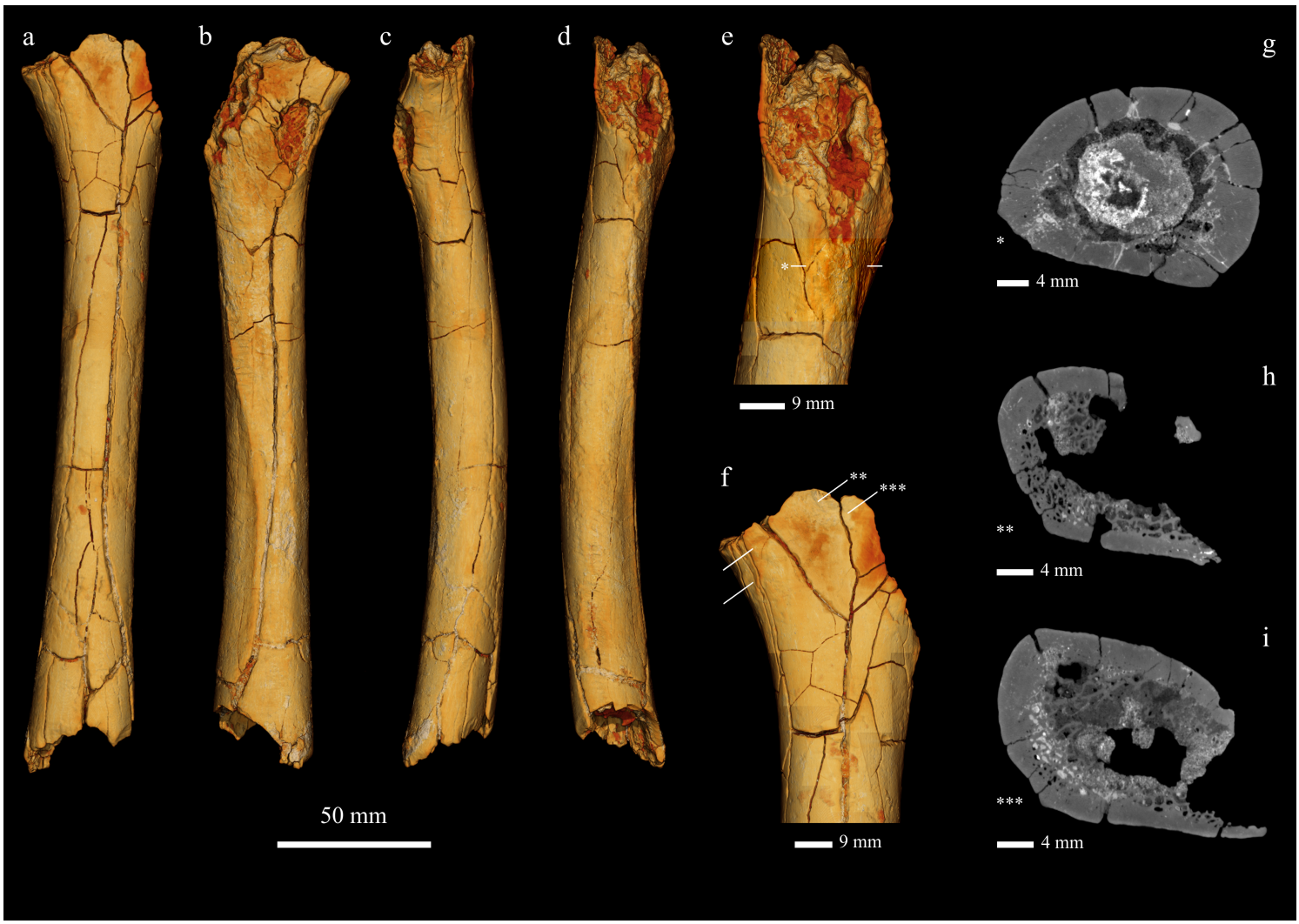

Figure 1

Femoral remain of S. tchadensis from late Miocene at Toros-Menalla 266th locality. Virtual representation of TM 266-01-063: a, anterior view; b, posterior view; c, medial view; d, lateral view; e, enlarged view of the proximal portion: e, lateral view; g, anterior view; microCT-slices at the level of the third trochanter (f); microCT-slices of the distal part of the femoral neck (g, h). The asterisks mark the microCT-slice levels and orientations.

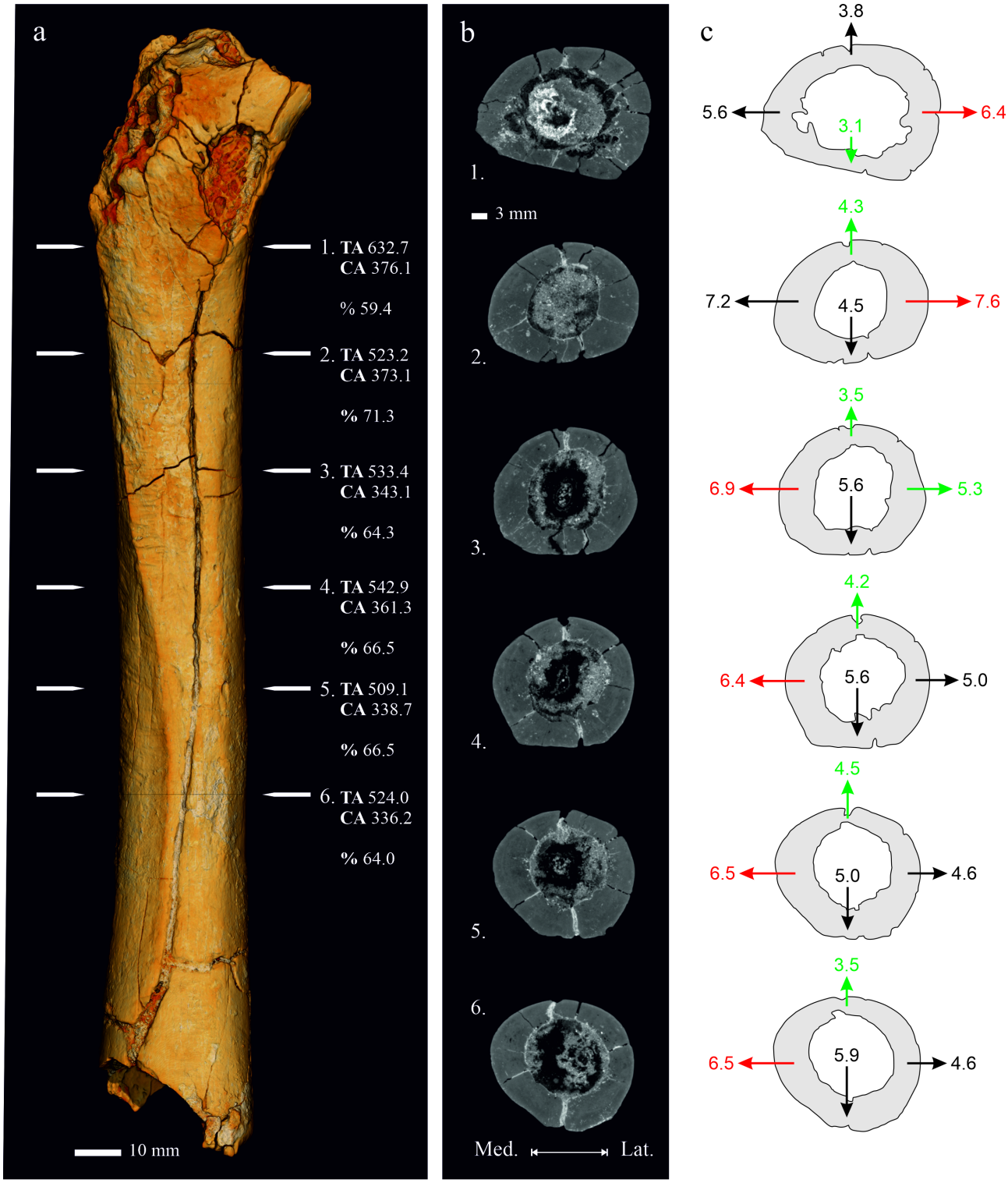

Figure 2

Cross-sectional geometric properties of the TM 266-01-063 femur. a, microCT-slice levels and corresponding percent of cortical area; b, microCT-slice images; c, interpretive drawings of the cortical thickness at microCT-slice levels, numbers are for the measured cortical thickness anteriorly, posteriorly, medially and laterally (in mm), maximum thickness is in red while minimum thickness is in green. TA, total area in mm2; CA, cortical area in mm2; %, percent of cortical area.

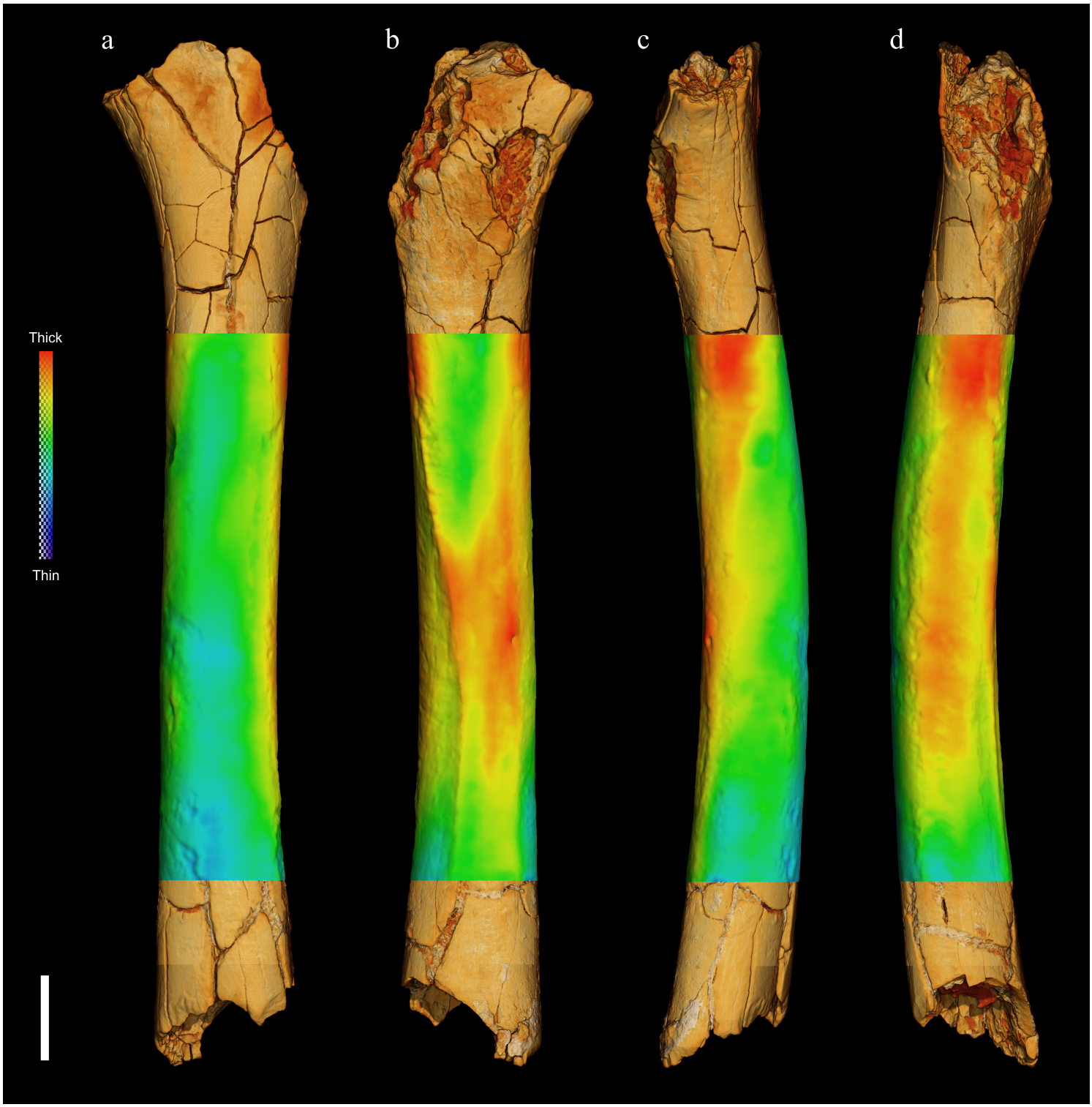

Figure 3

Three-dimensional cortical thickness of TM 266-01-063. a, anterior view; b, posterior view; c, medial view; d; lateral view. Scale bar is 20 mm. Chromatic scale corresponds to the look-up table of cortical thickness (in mm).

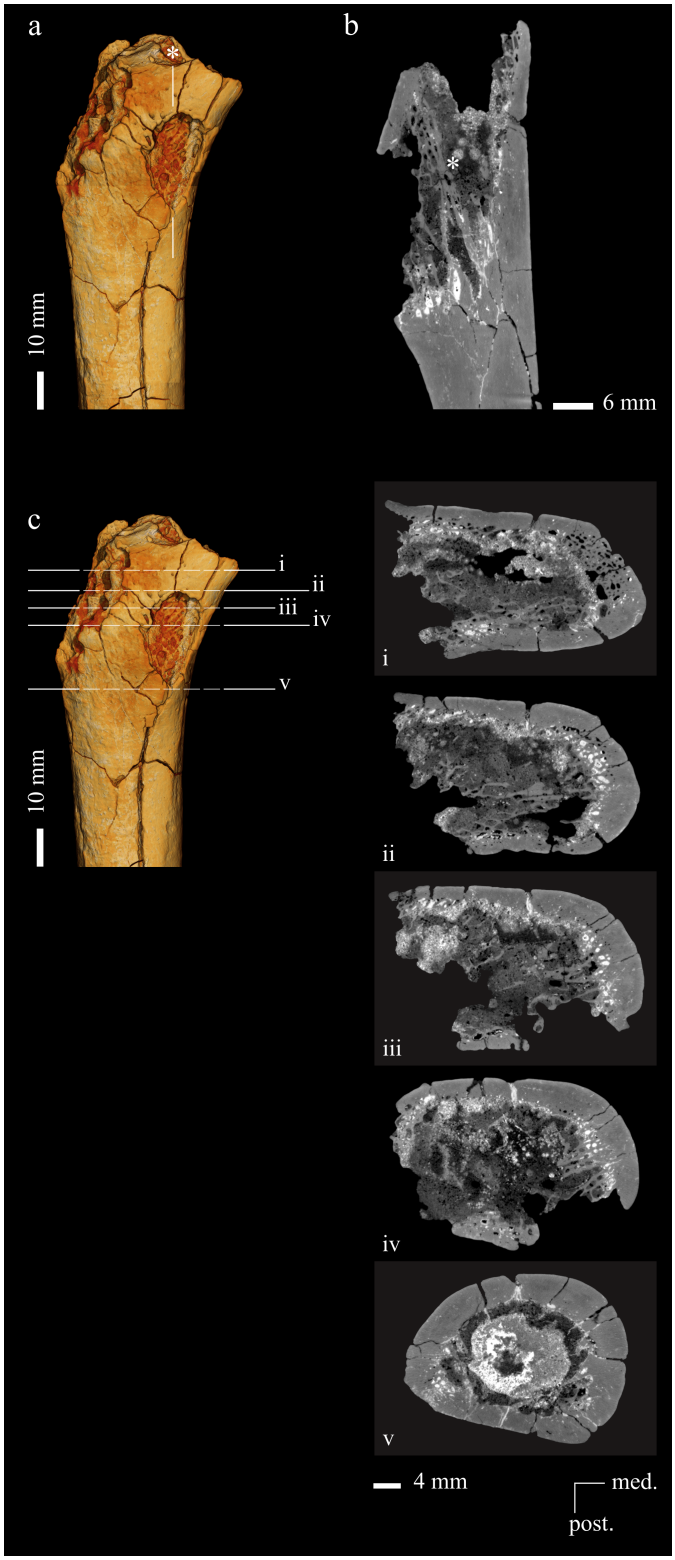

Figure 4

Illustration of the TM 266-01-063 calcar femorale. a, virtual representation of the proximal portion of the femur, posterior view; b, microCT-slice at the lesser trochanter level showing proximo-distal extension of

the calcar femorale (asterisk); c, virtual representation of the proximal portion of the femur showing microCT-slice levels and orientations; d, e, f, g, h, microCT-slice images for respectively slice levels from 1 to 5, showing expression of the calcar femorale transversally.

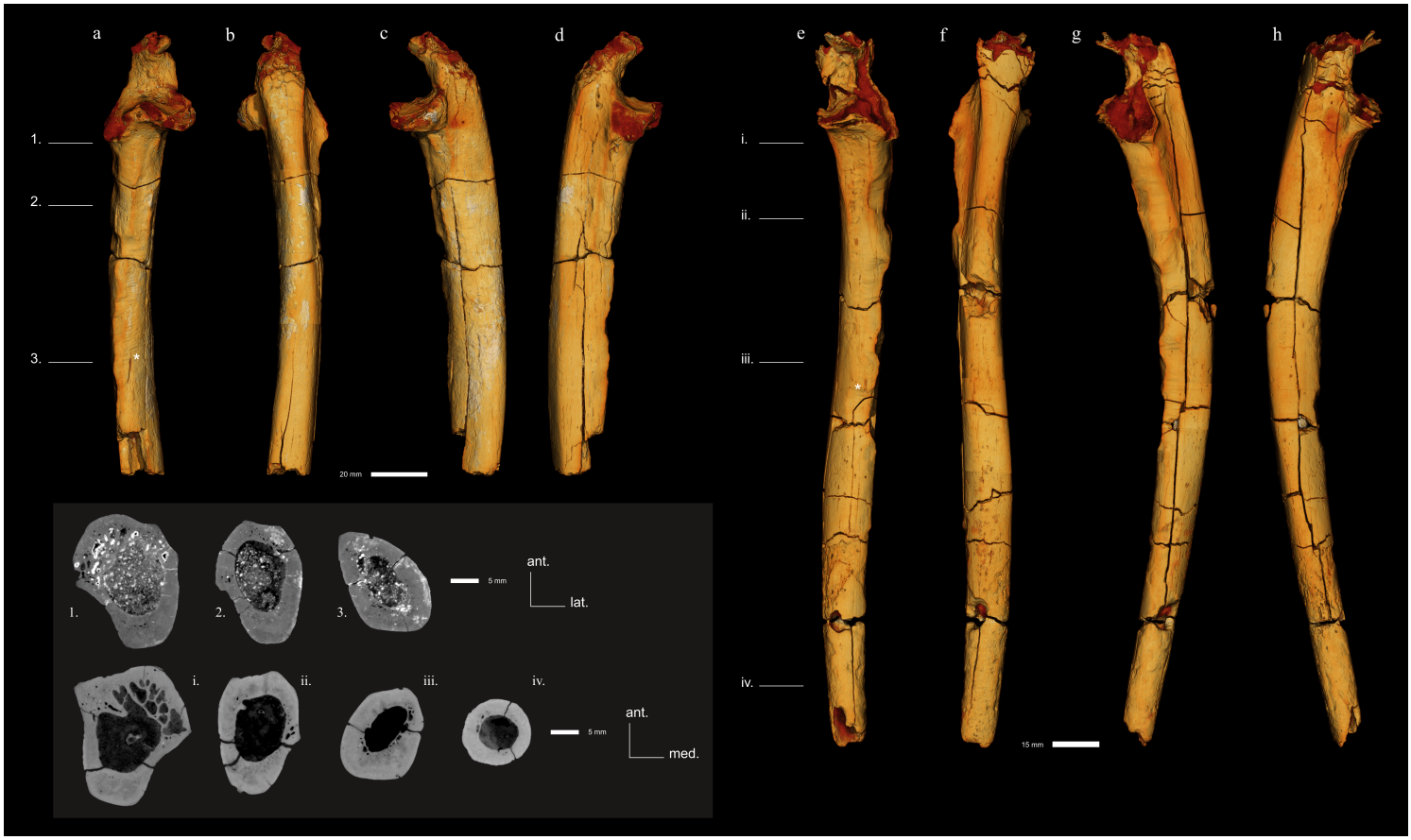

Figure 5

Ulnar remains of S. tchadensis from Late Miocene at Toros-Menalla 266 locality. TM 266-01-358: a, anterior view; b, posterior view; c, medial view; d, lateral view. TM 266-01-050: e, anterior view; f, posterior view; g, lateral view; h, medial view. MicroCT-slices images levels and orientations are numbered from 1 to 3 and i to iv respectively. The asterisks mark the location of the nutrient foramina.

Supplementary Files

This is a list of supplementary files associated with this preprint. Click to download.

- ExtData1.tif
- ExtData2.tif
- ExtData3.tif
- ExtData4.tif
- Supplementarynotes.docx
- SupplementaryTable1.xlsx